17th Brazilian Congress of Thermal Sciences and Engineering
November 25th-28th, 2018, Águas de Lindóia, SP, Brazil

ENCIT 2018-0180
COMPARISON BETWEEN TURBULENCE MODELS OVER MAGNUS EFFECT

Rodrigo Canestraro Quadros
Universidade Federal do Paraná. Av. Cel. Francisco H. dos Santos, 100 – Jardim das Américas, Curitiba – PR
rodrigocanes@gmail.com

Luciano Kiyoshi Araki
Universidade Federal do Paraná. Av. Cel. Francisco H. dos Santos, 100 – Jardim das Américas, Curitiba – PR
lucaraki@ufpr.br; lucianoaraki@gmail.com

Abstract. *Despite the benefits that can be obtained, and the growing number of studies carried out in recent years on the Magnus effect, no relevant studies on the response of this effect in simulations considering different turbulence models has been found. In this work, numerical investigations will be carried out on the observed effects on the behavior of stationary and rotating cylinders in a uniform flow field, considering the classical and widely applied turbulence models such as k-epsilon, k-omega, and its variant k-omega SST; generally called the RANS - Reynolds Average Navier-Stokes. Also, will be used the DES (Detached Eddy Simulation) modeling that combines the LES (Large Eddy Simulation) and RANS models. That is applied to zones of separation and highly adverse pressure gradient while this is used for the remaining flow. In addition to consider the different models, the dimensional scales that best meets the proposed problem will be verified. The simulations will be carried out for conditions of a Reynolds number 100 and 1000, for two-dimensional models, and the results will be compared with experimental data obtained in several other studies. The results have not been shown to be favorable solely to one model of turbulence.*

Keywords: *Magnus Effect, Turbulence Modeling, Turbulence Length-scale*

1. INTRODUCTION

A circular cylinder immersed in a free flow generates a fluid movement that has been the subject of many researches in the recent decades, from the point of view of theoretical analysis, experiments, and numerical simulations. The flow field generated under these conditions is equivalent to that obtained when a circular cylinder rotates and translates through a stationary fluid (Padrino and Joseph, 2006). This topic has also been approached in the research on boundary layer control and drag reduction over the last few years (Padrino and Joseph, 2006; Ece et al.,1984; He et al.,2000).

A rotating cylinder when exposed to a free flow will experience a simultaneous perpendicular force to its rotation axis and the direction of flow. This phenomenon is called the Magnus effect, named after the engineer Heinrich Gustav Magnus. The rotation of the cylinder has the characteristic of adding momentum to the fluid flow, which can be useful for several applications such as: control of the separation of the boundary layer in airfoils and lift in wind turbines. Thus, a device containing a rotating cylinder immersed in a free flow allows an active control of its fluid dynamics characteristics (Gada, 2016).

2. MAGNUS EFFECT

For the analysis of the Magnus effect, the two main parameters will be considered, which are the Reynolds number and the velocity ratio. The first parameter is defined by r – the cylinder radius, U – free flow velocity and ν - the kinematic viscosity of the fluid:

$$Re=2rU/\nu \tag{1}$$

The second parameter, the velocity ratio (α), is defined by r – the cylinder radius, ω – the angular velocity of the cylinder along its axisymmetric axis and U – the free flow velocity:

$$\alpha=\frac{r\omega}{U} \tag{2}$$

The velocity ratio is a dimensionless parameter that considers the ratio between the tangential velocity of the cylinder and the velocity of the free flow.

For the Magnus effect itself, Rayleigh, in his studies on the effects of lift, defined, for a cylinder immersed in an inviscid fluid, the following equations:

$$\Gamma=\oint v\cdot dl=v(2\pi r)=\omega r(2\pi r) \tag{3}$$

$$L=\rho U\Gamma=\rho U(2\pi\omega r^2) \tag{4}$$

where Γ is the circulation, v the tangential velocity, l the perimeter of the cylinder, L is the lift. The ratio between the lift term and the circulation is known as the Kutta-Joukowsky's relation and can be applied to any fluid dynamics profile, including airfoils, wings, and cylinders, as in the case of this study. For viscous fluids, such as air, the cylinder is also subject to pressure and viscous forces, which make the explanation more complex (Middendorf, 2003).

According to (Smith, 1979 apud Middendorf, 2003), the circulation in a real flow is not only the result of friction generated by fluid motion opposed to the average flow, which only occurs in a boundary layer very close to the surface. However, such movement of the fluid in the boundary layer affects the manner that the flow separates from the cylinder. The separation of the boundary layer occurs downstream of the side to which the cylinder accompanies the main flow, and upstream to the side at which the cylinder moves against the flow. Thus, the wake tends to move to the side where the cylinder is in opposition to the flow, causing deflection of the flow to that side, changes in the free flow and generating a resultant force in the rotating cylinder.

3. TURBULENCE MODELING

The study of turbulence models started with the need to predict the distribution of the average velocity or an average temperature field along a turbulent boundary layer. Due to the inability to represent such a phenomenon algebraically, some authors like Boussinesq and Prandtl used hypothesis to model the turbulent flow. Among the concepts introduced by them, there is the turbulent viscosity and the mixing length.

The turbulent viscosity, or eddy viscosity, proposed by Boussinesq, was taken like the molecular viscosity, in which turbulent stress acted similarly to viscous stress and thus, through this hypothesis, turbulent stress is proportional to velocity gradient. The mixing length, of Prandtl, is based on an analogy with the kinetic gases theory, in which the turbulent eddy, as well as gas molecules, are discrete entities and collide and exchange momentum at discrete time interval.

However, the use of the mixing length and the turbulent viscosity to solve problems related to turbulent flow were only possible if, in advance, it was possible to obtain the characteristic turbulent length scale. Both the algebraic models of, and the models of one differential equation are said incomplete, because they relate the turbulent length scale to a characteristic dimension of the flow, without, however, solving it.

The models of two differential equations such as k-Ω and k-ε are said complete, because they allow the calculation of the turbulent length scale, without knowing the structure of the flow in advance. The models of two equations have been the most used in the engineering area and in many research topics. From the model of two equations, several other models emerged with more differential equations for solving the closure problem, as well as transition models.

3.1 RANS – Reynolds Average Navier-Stokes: k-ε

The k-ε model is semi empirical and is based on the model of the transport equations for kinetic energy (k) and the dissipation rate (ε). Starting from the Navier-Stokes equations to obtaining the equations describing fluid movement and departing from the k-ε turbulence models, the transport equations are given by:

$$\frac{\partial}{\partial t}(\rho k)+\frac{\partial}{\partial x_i}(\rho k u_i)=\frac{\partial}{\partial x_j}\left[\left(\mu+\frac{\mu_t}{\sigma_k}\right)\frac{\partial k}{\partial x_j}\right]+G_k+G_b-\rho\varepsilon-Y_M+S_k \tag{5}$$

and

$$\frac{\partial}{\partial t}(\rho \varepsilon)+\frac{\partial}{\partial x_i}(\rho \varepsilon u_i)=\frac{\partial}{\partial x_j}\left[\left(\mu+\frac{\mu_t}{\sigma_\varepsilon}\right)\frac{\partial \varepsilon}{\partial x_j}\right]+C_{1\varepsilon}\frac{\varepsilon}{k}(G_k+C_{3\varepsilon}G_b)-C_{2\varepsilon}\rho\frac{\varepsilon^2}{k}+S_\varepsilon \tag{6}$$

and the turbulent viscosity is given by:

$$\mu_t=\rho C_\mu \frac{k^2}{\varepsilon} \tag{7}$$

where ρ the density of the fluid, k is the kinetic energy, ε is the dissipation rate, u_i the velocity of the flow in the i direction, G_k the generation of turbulence by kinetic energy and G_b, by buoyancy. σ_k and σ_ε represent the number of turbulent Prandtl and S_k and S_ω the source terms, if existing. The terms $C_{1\varepsilon}$, $C_{2\varepsilon}$, $C_{3\varepsilon}$, C_μ are constants.

3.2 RANS – Reynolds Average Navier-Stokes: k-ω

Starting from the Navier-Stokes equations to obtain the equations that describe the movement of the fluid and starting from the turbulence models k-ω, we have that the transport equations are given by:

$$\frac{\partial}{\partial t}(\rho k)+\frac{\partial}{\partial x_i}(\rho k u_i)=\frac{\partial}{\partial x_j}\left(\Gamma_k \frac{\partial k}{\partial x_j}\right)+G_k-Y_k+S_k \tag{8}$$

and

$$\frac{\partial}{\partial t}(\rho \omega)+\frac{\partial}{\partial x_i}(\rho \omega u_i)=\frac{\partial}{\partial x_j}\left(\Gamma_\omega \frac{\partial \omega}{\partial x_j}\right)+G_\omega-Y_\omega+S_\omega \tag{9}$$

where ρ is the density of the fluid, k is the kinetic energy, ui is the flow velocity in the direction i, Γ_k and ω is the effective diffusivity of k and ω, Y_k and Y_ω are the dissipation of k and ω and S_k and S_ω are the source terms, if existing. At the k-ω model the turbulent viscosity is implied to the effective diffusivity.

3.3 DES – Detached Eddy Simulation

According to Menter and Kuntz (2004), from a turbulence modeling point of view, it has been observed for a long time that the RANS (Reynolds Average Navier Stokes) models show some degree of unpredictability of the turbulent stresses in the decoupled shear layers emanating from the boundary layer separation line (Johnson et al., 1994). To improve the predictive capabilities of turbulence models for separation regions, Spalart (1997) proposed a hybrid approach, which combined RANS features with LES elements (Large Eddy Simulation). To this concept was given the name of DES (Detached Eddy Simulation). The principle of this model is to switch from RANS to LES in locations of separation and detachment. Strelets (2001) presented a model that combined the SST-RANS with the LES model for locations where the predicted turbulence length of the RANS model was greater than the mesh spacing of the model.

In the DES methodology, the dissipative term of the turbulent kinetic energy Y_k is changed to:

$$Y_k=\rho\beta^* k\omega f_{\beta^*} \rightarrow Y_k=\rho\beta^* k\omega F_{DES} \tag{10}$$

where β * is a coefficient for the dissipation calculation, f_{β^*} is an intermediate coefficient. FDES is expressed as:

$$F_{DES}=\max\left(\frac{L_t}{C_{des}\Delta_{max}},1\right) \tag{11}$$

where L_t is the turbulent length scale by the RANS model, given by:

$$L_t=\frac{\sqrt{k}}{\beta^*\omega} \tag{12}$$

The practical reason for choosing this type of formulation is that for the condition in which the DES model has the boundary layer attached to the body, the DES formulation becomes the same as RANS.

4. METODOLOGY

The numerical simulations for the determination of the appropriate turbulence models for the best description of the Magnus effect in a rotating cylinder were made as follows:

- Two-dimensional flow due to computational simplicity and application of the models, although the effects of turbulence on the wake formed after the cylinder are three-dimensional;
- RANS k-ε and k-ω, and DES turbulence models with RANS SST k-ω formulation;
- Reynolds number of the mean free flow of 100 and 1000;
- Variable length scales;
- Fluid: air;
- Ratio of dimensionless velocities 0 and 6;
- ANSYS FLUENT 18.1 commercial software;
- Discretization by finite volume method;
- SIMPLE (Semi-Implicit Method for Pressure-Linked Equations) pressure-velocity coupling method;
- Time-step required for unitary CFL (Courant-Friedrich-Lewis) condition.
- Simulation time of 30 s to Re~100 and 2 s to Re~1000;
- Discretization of second order for all terms;

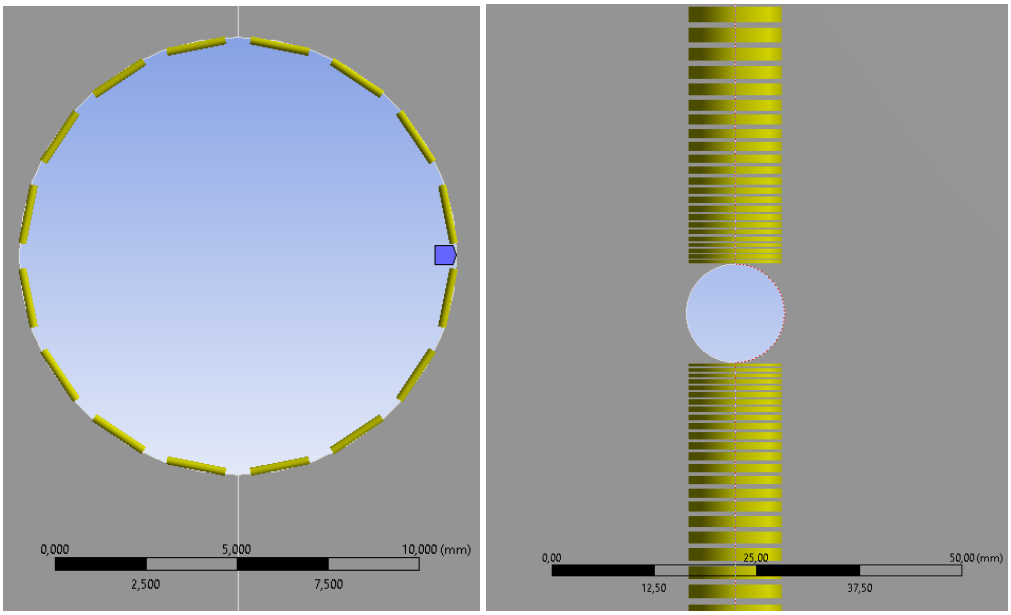

Figure 1. Circumferential mesh division (on the left) and radial mesh division (on the right)

Figure 1 shows the mesh division. The discretization of the two-dimensional simulation mesh was done using a variable-sized mesh, being smaller for elements close to the cylinder and larger away from it, in the radial orientation. For the definition of the size of the elements, a division of the cylinder circumference was elaborated into a growing number of elements, initiated by 16 elements, and increasing up to 1024 in a geometric ratio equivalent to two. The same was done in the radial direction, which the growth rate of the elements followed, also, a geometric ratio. The number of divisions, growth ratio, and the size of the first element are shown in Tab 1.

Table 1. Number of division, growth ratio and the first element size used in the numerical simulation

	No. Of Division	Growth Ratio	1st Element Size
1	16	1,3004 (30,04%)	2,356 mm
2	32	1,1405 (14,05%)	1,178 mm
3	64	1,0680 (6,80%)	0,589 mm
4	128	1,0334 (3,34%)	0,295 mm
5	256	1,0166 (1,66%)	0,147 mm
6	512	1,0083 (0,83%)	0,074 mm
7	1024	1,0041 (0,41%)	0,037 mm

Figure 2 shows the mesh division for the case of 128 divisions.

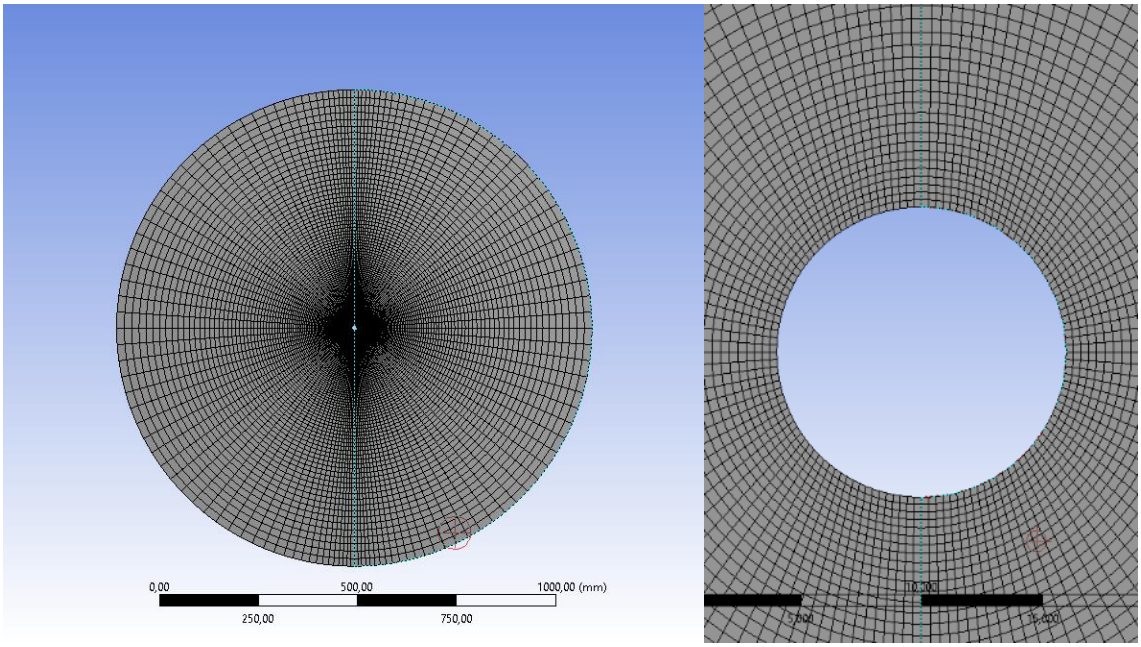

Figure 2. Mesh with 128 divisions on circumferential and radial direction

5. RESULTS

The results of the numerical simulations will be presented for flows with Reynolds number equivalent to 100 and 1000. The values of the drag and lift coefficients will be presented to cylinders, which the velocity ratio is 0 and 6. In addition to the dimensionless coefficients, a correlation between the different models of turbulence will be presented, as well as the variation in the number of Strouhal according to the Reynolds number

5.1 Reynolds number 100 – velocity ratio 0

For a flow whose Reynolds number is equivalent to 100, it is shown in Fig. 3 the comparison between the drag and lift coefficients, over time, for different models of turbulence.

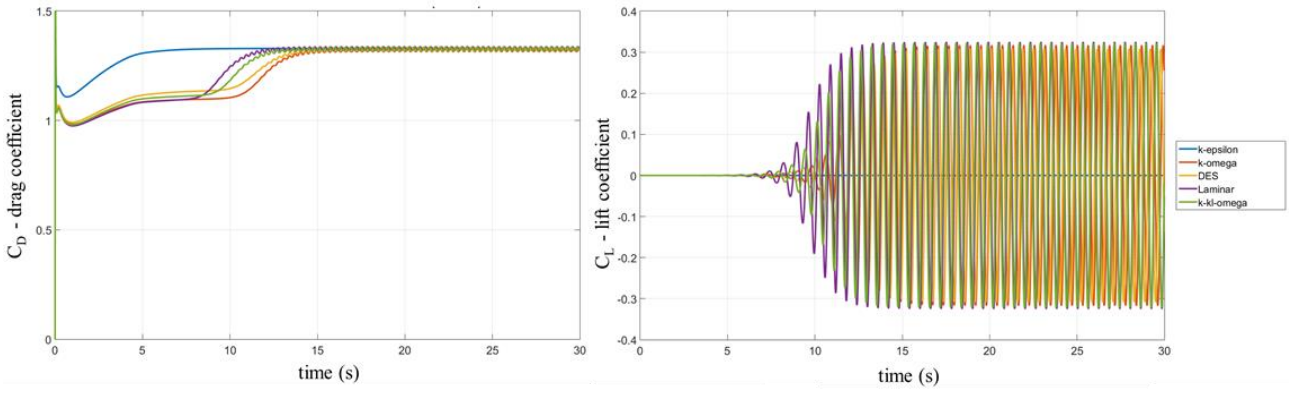

Figure 3. Drag (left) and Lift (right) coefficient over a flow with Reynolds number 100 and velocity ratio 0.

In Tab. 2 the comparations between the results obtained numerically, in this work, and the results obtained by other authors is presented. It is observed that the average value of the drag coefficient is similar to all the models presented, only differs in the oscillatory value. For the k-ε model there is no oscillation in the value of the drag coefficient.

Table 2. Mean and oscillatory drag coefficient – Re~100 and α=0

	$\overline{C_D} \pm C_{D_{osc}}$ for Re~100 (α=0)
k-ϵ Realizable	1,32912 ± 0,00000
k-ω SST	1,32197 ± 0,00841
DES	1,32716 ± 0,00829
Laminar	1,32899 ± 0,00930
k-kl-ω	1,32640 ± 0,00907

	$\overline{C_D} \pm C_{D_{osc}}$ para Re 100 (α=0)
Rusell; Wang (2003)	1,380 ± 0,007
Calhoun; Wang (2002)	1,350 ± 0,014
Braza et al. (1986)	1,386 ± 0,015
Choi et al. (2007)	1,340 ± 0,011
Liu et al. (1998)	1,350 ± 0,012
Guerrero (2009)	1,380 ± 0,012

The comparison between the results of the lift coefficient is presented in Tab 3. As the drag coefficient, for Reynolds 100 and zero velocity ratio, the k-ε model does not present oscillation.

Table 3. Mean and oscillatory lift coefficient – Re~100 and α=0

	$\overline{C_L} \pm C_{L_{osc}}$ for Re~100 (α=0)
k-ϵ Realizable	0,00000 ± 0,00000
k-ω SST	0,00000 ± 0,31731
DES	0,00000 ± 0,30838
Laminar	0,00000 ± 0,32506
k-kl-ω	0,00000 ± 0,32209

	$\overline{C_L} \pm C_{L_{osc}}$ for Re~100 (α=0)
Rusell; Wang (2003)	0,000 ± 0,322
Calhoun; Wang (2002)	0,000 ± 0,300
Braza et al. (1986)	0,000 ± 0,250
Choi et al. (2007)	0,000 ± 0,315
Liu et al. (1998)	0,000 ± 0,339
Guerrero (2009)	0,000 ± 0,333

5.2 Reynolds number 1000 – velocity ratio 0

For a flow whose Reynolds number is equivalent to 1000, the comparison between the drag and lift coefficients over time for different models of turbulence is shown in Fig. 4.

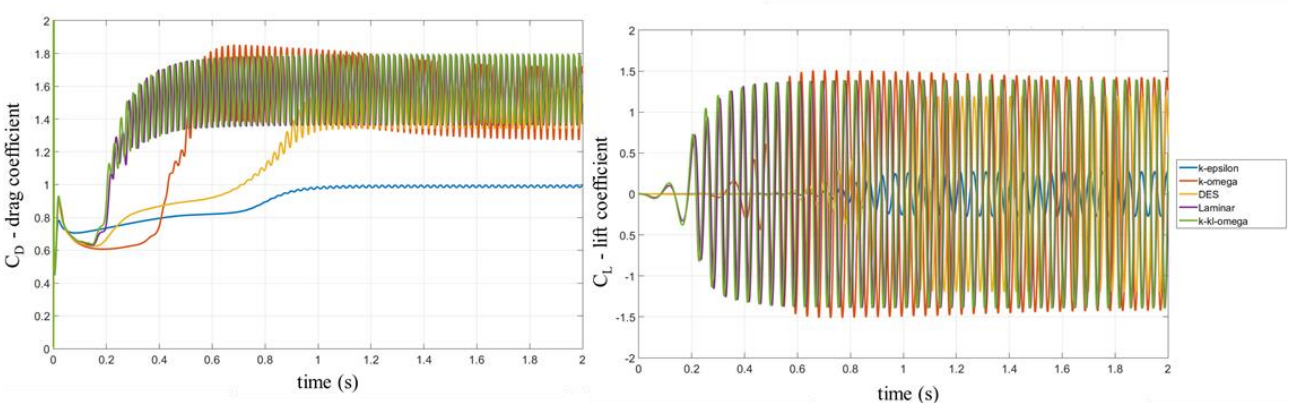

Figure 4. Drag (left) and Lift (right) coefficient over a flow with Reynolds number 1000 and velocity ratio 0.

Table 4. Mean and oscillatory drag coefficient – Re~1000 and α=0

	$\overline{C_D} \pm C_{D_{osc}}$ for Re~1000(α=0)
k-ϵ Realizable	0,98968 ± 0,00773
k-ω SST	1,50902 ± 0,23800
DES	1,46699 ± 0,12697
Laminar	1,57511 ± 0,21434
k-kl-ω	1,58305 ± 0,21549

	$\overline{C_D} \pm C_{D_{osc}}$ for Re~1000(α=0)
Singh; Mittal (2005)	0,98
Rosetti et al. (2012)	0,99
Rahman et al. (2007)	0,995
Anderson (2005)	0,9

In Tab. 4 and Tab. 5 the comparisons between the drag and lift coefficients for the different turbulence models used are presented, and it is also presented the comparison between the data obtained in this work and by other authors.

Table 5. Mean and oscillatory lift coefficient – Re~1000 and α=0

	$\overline{C_L} \pm C_{L_{osc}}$ for Re~1000 (α=0)
k-ϵ Realizable	0,00000 ± 0,27629
k-ω SST	0,00212 ± 1,44131
DES	0,00000 ± 1,19675
Laminar	0,00000 ± 1,39201
k-kl-ω	0,00000 ± 1,39898

	$\overline{C_L} \pm C_{L_{osc}}$ for Re~1000 (α=0)
Rahman et al. (2007)	0,00 ± 0,23

5.3 Comparison Between Reynolds number 100 and 1000 – velocity ratio 0

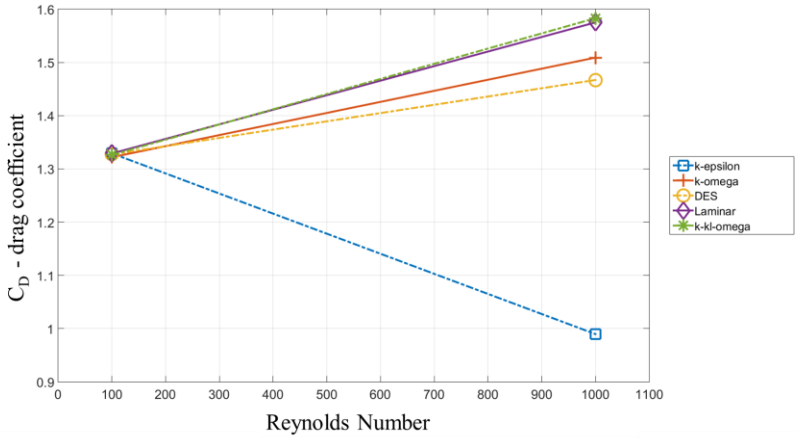

Figure 5. Drag coefficient over different Reynolds number

In Fig. 5 and Fig 6, the comparison, respectively, between the average drag coefficient and the number of Strouhal for the different Reynolds numbers is shown. In this case, the velocities ratio is null.

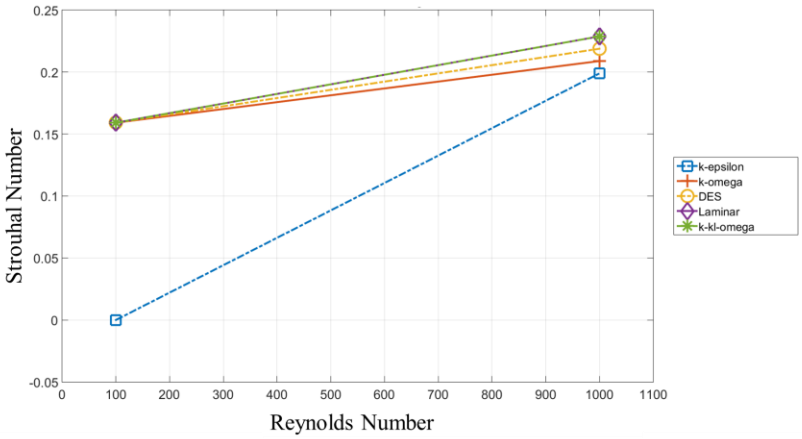

Figure 6. Relationship between Strouhal and Reynolds number

5.4 Reynolds number 100 – velocity ratio 6

For a flow whose Reynolds number is equivalent to 100, the comparison between the drag and lift coefficients over time for different models of turbulence is shown in Fig. 7. The velocities ratio between the angular velocity of the cylinder and the velocity of the flow is 6.

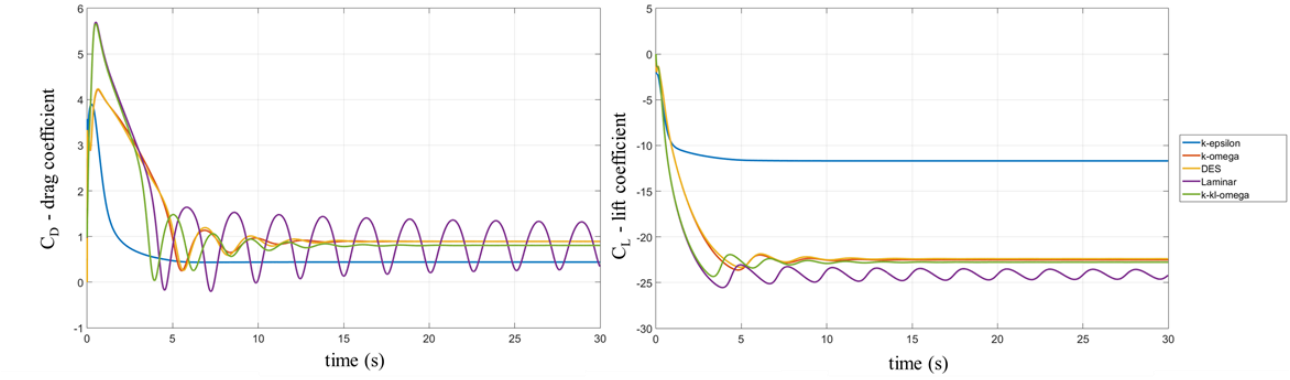

Figure 7. Drag (left) and Lift (right) coefficient over a flow with Reynolds number 100 and velocity ratio 6.

In Tab. 6 the results obtained for the different models of turbulence, both for the drag and lift coefficients, are presented. The studies carried out by other authors in this area are limited to a few data obtained numerically.

Table 6. Mean and oscillatory drag coefficient – Re~100 and α=6 (left) and mean and oscillatory lift coefficient – Re~100 and α=6 (right).

	$\overline{C_D} \pm C_{D_{osc}}$ for Re~100 (α=6)
k-ϵ Realizable	0,44017 ± 0,00000
k-ω SST	0,89279 ± 0,00033
DES	0,89375 ± 0,00099
Laminar	0,78911 ± 0,55733
k-kl-ω	0,80619 ± 0,00174

	$\overline{C_L} \pm C_{L_{osc}}$ for Re~100 (α=6)
k-ϵ Realizable	−11,68570 ± 0,00000
k-ω SST	−22,51390 ± 0,00032
DES	−22,39010 ± 0,00094
Laminar	−24,09330 ± 0,56128
k-kl-ω	−22,76880 ± 0,00159

The average values of the lift coefficient for Reynolds 100 and velocity ratio equivalent to 6 do not have direct data in the bibliography, however, through interpolated data from literature, the expected absolute value of the lift coefficient is between 20 and 25. Which leaves the k-ε model away from the expected value. The value of the drag coefficient is not shown in the literature, for this case, however, by the proximity between the values of the lift coefficient for the model k-Ω and DES to the data obtained in the literature, and by the similarity between the absolute values for the drag coefficient, it is estimated that the data for these models are closer to the reality.

6. CONCLUSIONS

Among the models used, for simulated conditions, it is not possible to say that there is only a single model capable of representing the flow around the cylinder. In this way, it is observed that, although it represents a seemingly simple problem, the flow around a cylinder is complex. This is evident when it takes into consideration that several Reynolds values can lead to different flow regimes, ranging from virtually inviscid (lower Reynolds – next to Unit O(0)), to the complete transition to the turbulent regime (Reynolds O(6)), going through almost a dozen different combinations.

For the study carried out, models based on the k-Ω formulation obtained better results for the conditions in which the Reynolds number is close to 100. Although the number of Reynolds is low, and the flow is laminar from the boundary layer to the wake, it is proved that even for values of low turbulent viscosity, satisfactory results are obtained with models k-Ω and DES. This no longer occurs for a number of Reynolds 1000, when the flow is laminar in the boundary but turbulent on the wake. This is because the turbulence occurs only in the free shear flow (wake), a condition in which the k-ε model can better represent. Even for the model DES that uses the SST (shear stress transport), no good results are obtained, because although it is a mixed model between k-ε (free flow) e k-ω (proximity to the wall), is not able to properly represent the turbulent flow.

7. REFERENCES

ANDERSON, J. D. Fundamentals of Aerodynamics. 4th ed. Columbus, USA: McGraw-Hilll, 2005.

BRAZA, M.; CHASSAING, P.; HINH, H. Numerical Study And Physical Analysis Of The Pressure And Velocity Fields In The Near Wake Of A Circular Cylinder. Journal of Fluid Mechanics, p. 79–130, 1986.

CALHOUN, D.; WANG, Z. A Cartesian Grid Method For Solving The Two-Dimensional Streamfunction-Vorticity Equations In Irregular Regions. Journal of Computational Physics, p. 231–275, 2002.

CHOI, J.; OBEROI, R.; EDWARDS, J.; ROSATI, J. An Immersed Boundary Method For Complex Incompressible Flows. Journal of Computational Physics, p. 757–784, 2007.

ECE, M. C.; WALKER, J. D. A.; DOLIGALSKI, T. L. The boundary layer on an impulsively started rotating and translating cylinder. Physics of Fluids, v. 27, n. 5, p. 1077, 1984.

GADA, K.; RAHAI, H. Lift and drag forces of a high efficiency airfoil with an embedded rotating cylinder. ASME International Mechanical Engineering Congress and Exposition, Proceedings (IMECE), v. 7, p. 1–8, 2016.

GUERRERO, J. Numerical Simulation Of The Unsteady Aerodynamics Of Flapping Flight, 2009. University of Genoa.

HE, J. W.; GLOWINSKI, R.; METCALFE, R.; NORDLANDER, A.; PERIAUX, J. Active Control and Drag Optimization for Flow Past a Circular Cylinder: I. Oscillatory Cylinder Rotation. Journal of Computational Physics, v. 163, n. 1, p. 83–117, 2000.

LIU, C.; ZHENG, X.; SUNG, C. Preconditioned Multigrid Methods for Unsteady Incompressible Flows. Journal of Computational Physics, p. 33–57, 1998.

MENTER, F. R.; KUNTZ, M. Adaptation of Eddy-Viscosity Turbulence Models to. Lecture Notes in Applied and Computational Mechanics, v. 19, p. 339–352, 2004.

MIDDENDORF, J. CFD Modeling of Wind Tunnel Flow over a Rotating Cylinder John Middendorf Student Number 3049731 Computation Fluid Dynamics Professors Tracie Barber / Eddie Leonardi signed. Fluid Dynamics, n. 3049731, 2003.

PADRINO, J. C.; JOSEPH, D. D. Numerical study of the steady-state uniform flow past a rotating cylinder. 2006.

RAHMAN, M.; KARIM, M.; ALIM, A. Numerical Investigation Of Unsteady Flow Past A Circular Cylinder Using 2-D Finite Volume Method, v. M, n. 1997, 2007.

ROSETTI, G. F.; VAZ, G.; FUJARRA, A. L. C. URANS Calculations for Smooth Circular Cylinder Flow in a Wide Range of Reynolds Numbers: Solution Verification and Validation. Volume 5: Ocean Engineering; CFD and VIV, p. 549, 2012.

RUSELL, D.; WANG, Z. A Cartesian Grid Method for Modeling Multiple Moving Objects in 2D incompressible viscous flow. Journal of Computational Physics, p. 177–205, 2003.

SINGH, S. P.; MITTAL, S. Flow past a cylinder: Shear layer stability and drag crisis. Int. J. Numer. Meth. Fluids, v. 47, p. 75–98, 2005.

8. RESPONSIBILITY NOTICE

The authors are the only responsible for the printed material included in this paper.